Biochemical Pharmacology 201 (2022) 115095

Contents lists available at ScienceDirect

Biochemical Pharmacology

journal homepage: www.elsevier.com/locate/biochempharm

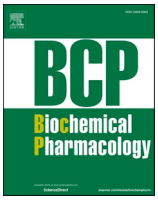

Targeted delivery of a colchicine analogue provides synergy with ATR inhibition in cancer cells

Francis M. Barnieh *, Goreti Ribeiro Morais, Herbie Garland, Paul M. Loadman, Robert A. Falconer *

Institute of Cancer Therapeutics, Faculty of Life Sciences, University of Bradford, Bradford BD7 1DP, U.K

ARTICLE INFO

Keywords:
MT1-MMP
Colchicine
ICT2588
AZD6738
ATR

ABSTRACT

Despite significant preclinical promise as anticancer agents, vascular-disrupting agents have yet to fulfil their clinical potential due to systemic toxicities. ICT2588 is a tumour-selective MT1-MMP-targeted prodrug of azademethylcolchicine, ICT2552. We investigate activation of ICT2588 and subsequent release of ICT2552 in tumour cells, and examine its ability to induce G2/M cell cycle arrest. We also explore synergism between ICT2588 and ATR inhibition, since colchicine, in addition to its vascular-disrupting properties, is known to induce G2/M arrest, DNA damage, and trigger apoptosis. Several ATR inhibitors are currently undergoing clinical evaluation. The cellular activation of ICT2588 was observed to correlate with MT1-MMP expression, with selective release of ICT2552 not compromised by cellular uptake and prodrug activation mechanisms. ICT2588 induced G2/M arrest, and triggered apoptosis in MT1-MMP-expressing cells, but not in cells lacking MT1-MMP expression, while ICT2552 itself induced G2/M arrest and triggered apoptosis in both cell lines. Interestingly, we uncovered that the intracellular release and accumulation dynamics of ICT2552 subsequent to prodrug activation provided synergism with an ATR inhibitor in a way not observed with direct administration of ICT2552. These findings have important potential implications for clinical combinations of ICT2588 and DNA repair inhibitors.

1. Introduction

Vascular disrupting agents (VDAs) are an effective chemotherapeutic class of anticancer agent that target established tumour vasculature, which differs significantly from normal vasculature, through disruption of microtubule dynamics. Microtubules play an important role in the maintenance of vascular integrity, hence the ability of these agents to collapse tumour vasculature and consequently cause tumour necrosis [1,2]. Besides their vascular disrupting properties, tubulin-targeted agents have also been reported to induce G2/M arrest, DNA double strand damage, and to trigger apoptosis [3–5] in tumour cells. VDAs, exemplified by colchicine and analogues, ZD6126 and the combretastatins, have demonstrated significant preclinical therapeutic potential, but have yet to fulfil this promise in the clinic, due to off-target toxicities, and notably cardiotoxicity [6,7].

ICT2588 is a tumour-targeted prodrug of the potent colchicine analogue, azademethylcolchicine (ICT2552), designed to be selectively activated (cleavage of the glycine-homophenylalanine bond of ICT2588 following recognition of the peptide sequence) by the protease MT1-MMP found in solid tumours and tumour blood vessels [8,9]. Previous reports have demonstrated the preclinical efficacy of ICT2588, and evidence for reduced systemic exposure and associated toxicity of the colchicine warhead (cardiotoxicity in particular), as a result of its metabolic stability in plasma and normal tissues, with tumour-selective activation accounting for its anti-tumour activity [8–10]. Preclinical studies with ICT2588 have to-date focused on its *ex-vivo* metabolism, selective tumour vascular disrupting ability, and subsequent anti-tumour activity *in vivo* [8,9]. Cellular activation and metabolism of ICT2588, and related effects on mechanisms associated with cell cycle arrest at the G2/M phase and induction apoptosis remain to be explored.

DNA Damage Response (DDR) signalling pathways have in recent times gained significant attention in cancer therapy, with inhibitors of DDR proteins including ATR, ATM, DNA-PK, CHK1, CHK2, Wee1, and PARP currently at various stages of preclinical and clinical development

Abbreviations: ATR, Ataxia telangiectasia and Rad3 related kinase; MT1-MMP, Membrane type 1 matrix metalloproteinase; VDA, Vascular disrupting agent; DDR, DNA Damage Response; HSA, Highest single agent; ZIP, Zero interaction potency.

* Corresponding authors.
E-mail addresses: f.mprahbarnieh1@bradford.ac.uk (F.M. Barnieh), r.a.falconer1@bradford.ac.uk (R.A. Falconer).

https://doi.org/10.1016/j.bcp.2022.115095
Received 30 March 2022; Received in revised form 13 May 2022; Accepted 13 May 2022
Available online 20 May 2022

[11,12]. Ataxia telangiectasia and Rad3- related protein (ATR) is one of the main regulators of the DDR pathway that coordinates cellular responses to a broader spectrum of DNA damage [13]. The crucial roles for ATR in DDR are particularly implicated at the S and G2/M phases of the cell cycle [14], with emerging evidence now suggesting inhibition of ATR in the presence of DNA damaging agents and cell cycle inhibitors to be attractive therapeutic strategies [15–17]. Inhibition of ATR in the presence of a DNA damaging agent (e.g. cytotoxic chemotherapy) prevents activation of the DDR in response, leading to a lethal accumulation of DNA damage that as a result potentiates the anti-tumour effects of these agents, resulting in a highly effective combination therapy strategy.

In this study, we have investigated the activation of ICT2588 in cancer cells, examined its G2/M cell cycle arrest potential, and explored mechanisms of synergy between ICT2588 and a potent ATR inhibitor (AZD6738, ceralasertib) currently undergoing clinical evaluation. We show that, consistent with the previously reported *ex-vivo* metabolism of ICT2588, the prodrug is selectively metabolised by MT1-MMP expressing cells, and induces G2/M arrest and apoptosis in these cells. We further demonstrate the generation of significant DNA damage (double-strand breaks) and subsequent induction of apoptosis following ATR inhibition by AZD6738 in the presence of ICT2588 treatment, particularly at low and non-toxic concentrations of both agents. These findings have important potential implications for both agents, and suggest that combinations of ICT2588 and DNA damage repair inhibitors are likely to be advantageous as both agents head towards the clinic.

2. Materials and methods

2.1. Materials

Azademethylcolchicine (ICT2552) and ICT2588 were synthesised and purified at the Institute of Cancer Therapeutics, U.K. as previously described [8]. AZD6738 was purchased from Euroasia Chemicals, India. RPMI-1640 media, phosphate buffered saline (PBS), protease inhibitors and DMSO were each purchased from Merck, U.K. FxCycle™ PI/RNase staining solution (ThermoFisher, U.K.). Antibodies for p-ATR (2853), p-CHK1$^{(S345)}$ (2348), CHK1 (2360), PARP/cleaved PARP (9532), β-actin, horseradish peroxidase (HRP)–conjugated anti-rabbit and anti-mouse secondary antibodies were obtained from Cell Signalling Technology, U.K. MT1-MMP antibody (clone LEM-2/15.8) was obtained from Merck, U.K. Anti-gamma H2AX and anti-mouse IgG H&L (Alexa Fluor® 488) were purchased from Abcam, U.K. All other chemicals were of analytical grade.

2.2. Cell culture

Human breast carcinoma (MCF-7), human breast adenocarcinoma (MDA-MB-231) and fibrosarcoma (HT1080) cell lines were obtained from American Type Culture Collection (ATCC). Cells were cultured in RPMI-1640 supplemented with 10% (v/v) foetal bovine serum, sodium pyruvate (1 mM), and L-glutamine (2 mM) in a humidified incubator at 37 °C with 5% of carbon dioxide. Cell lines were used at low passage (<12 passages) for<6 months.

2.3. Western blotting

Cell pellets were lysed by resuspension in RIPA buffer with protease inhibitors, and incubated on ice for 30 min, sonicated and centrifuged (10,000 g, 10 min, 4 °C). Supernatants were pipetted, and total protein concentrations determined using a BCA protein assay kit (Thermo Fisher Scientific, UK). Protein (40 μg) of total cell lysate was separated by 4–15% Mini-PROTEAN TGX Gels (Bio-Rad, UK) and then transferred onto nitrocellulose membranes. Membranes were blocked with 5% dry milk in TBST. Membranes were probed for specific protein expression with respective antibodies, followed by horseradish peroxidase (HRP)-conjugated secondary antibodies. These immunoblots were visualised and analysed using ChemiDoc Imaging System with Image Lab Software 6.1.

2.4. In vitro metabolism of ICT2588

Cellular activation and metabolism of ICT2588 was conducted as described previously [18], with slight modifications. Cells (1×10^6/ml) in complete media were pipetted into Eppendorf tubes (1 per time point plus controls), and centrifuged (1000 g, 5 min) to pellet cells, with media removed. Pre-warmed media (1 ml) containing either ICT2552 or ICT2588 (10 μM) were added to each Eppendorf tube. Controls contained either no cells or no drug. Samples were incubated for 0, 5, 10, 30, and 60 min at 37 °C. At each time point samples were centrifuged (1000 g, 2 min), and the resulting cell pellet washed (twice) with ice-cold PBS. Cell pellets were solubilised in acetonitrile (200 μl), and then sonicated to disrupt the cells. Samples were centrifuged (10000 g, 10 min), with the supernatant collected. Supernatants were then dried using a SP Genevac EZ-PLUS evaporator for 30 min. The dried reaction was dissolved in a solution of 90% MeOH, 10% H_2O, 0.1% formic acid (50 μl), which was then transferred into an HPLC vial for LC-MS analysis.

2.5. LC-MS based metabolism assay

Stock solutions of ICT2552 and ICT2588 were prepared at 10 mM in DMSO and stored at −20 °C. Standard solutions for system calibration were made by further dilutions of stock solutions with a mixture of 10 % mobile phase A (MPA) and 90 % mobile phase B (MPB). For each set of experiments run on LC-MS, calibration curves were created between 0.1 μM and 2 μM. LC-MS of samples was carried out using a gradient method described below using a HiChrom RPB column (25 cm × 2.1 mm id; HIRPB-250AM; R6125) on a Waters Alliance 2695 HPLC (Micromass, Manchester, UK) with a photodiode array detector, connected in series with a Waters Micromass ZQ quadrupole mass spectrometer in ESI^+ mode. ICT2588 and its respective metabolites, including ICT2552, were analysed using UV absorbance at 360 nm, and set single ion recordings. Samples were maintained at 4 °C in the auto-sampler and 10 μl was injected for analysis. Cellular drug concentrations were diluted at the end of the experiment in 50 μl MPB. Thus, to determine the actual concentration of drug in the cell pellets, the following equation was applied (all volumes in μl): Dilution factor = [(volume of a single cell × 1×10^6 cells) + 50 μl] / volume of a single cell × 1×10^6 cells. Raw LC-MS data were processed using Mass Lynx V4.1. Graphs were plotted using Graph Pad Prism 8.

MS ESI + source parameters: Desolvation gas; 650 l/h, cone gas; 50 l/h, capillary voltage; 3 kV, extraction voltage; 5 V, cone voltage; 20 V, Rf voltage; 0.2 V, source block temperature; 120 °C and desolvation temperature; 350 °C.

Gradient method.

Time (min)	MPA (%)	MPB (%)
0	60	40
15	40	60
25	0	100
26	60	40

Run Time = 35 min; Injection Vol = 10 μl.

2.6. Cell cycle analysis

MCF-7 and HT1080 cells were seeded at a density of 5×10^5 cells and incubated for 24 h. Cells were treated with compounds for 24 h and 72 h. Treated cells and controls were trypsinised, washed with PBS, and fixed with 66.6% ethanol overnight. The fixed cells were rinsed with PBS, labelled with FxCycle™ PI/RNase staining solution following the manufacturer's instructions (Thermo Fisher Scientific, UK), and analysed by

flow cytometry (BD Accuri C6 Plus Flow Cytometer).

2.7. MTT assay

In vitro chemosensitivity of cells to compounds was determined using the 3-(4,5-dimethylthiazol-2-yl)-2,5-diphenyltetrazolium bromide (MTT) assay. Cells (5.0×10^3/well) were seeded in 96-well plates and incubated overnight at 37 °C with 5% CO_2. Cells were treated with increasing concentrations of AZD6738, ICT2588, and ICT2552 or solvent (DMSO) for 24, 48 and 96 h. DMSO concentrations did not exceed 0.1%, which was not toxic at this concentration. After compound treatment, the chemosensitivity of the cells was assessed, and cell survival post-treatment determined. Survival curves were obtained and IC_{50} values calculated using GraphPad Prism 8.

3. Results

3.1. MT1-MMP expression correlates with ICT2588 metabolism

The expression of MT1-MMP in human cancer cell lines has been reported previously, with fibrosarcoma cell line (HT1080) and breast carcinoma cell line (MCF-7) identified as reliable positive and negative tumour cells for active MT1-MMP protein expression respectively [8]. We assessed the expression of MT1-MMP in HT1080 and MCF-7 cells using western blotting (Fig. 1A), flow cytometery (Fig. 1B) and immunofloresence techniques (Data not shown). A specific band (57 kDa) corresponding to active MT1-MMP was detected in HT1080, but not in MCF-7 cells Fig. 1A), which is consistent with earlier studies [8,19]. Similar results were observed using flow cytometry (Fig. 1B).

HT1080 cells (MT1-MMP positive) and MCF-7 cells (MT1-MMP negative) were used to examine the role of MT1-MMP expression in ICT2588 activation and metabolism. The cellular activation of ICT2588 and subsequent intracellular concentration of the released active aza-demethylcolchicine "warhead" ($ICT2552^{act}$) were assessed using an LC-MS based metabolism assay (Fig. 1C). As shown in Fig. 1D, a time-dependent release of the active warhead was observed in HT1080 cells contrary to the negligible release in MCF-7 cells which reflects the differential activation of ICT2588 by these cells. This differential activation was observed to account for more than a 10-fold increase in $ICT2552^{act}$ concentration in HT1080 cells (Fig. 1E). The rate of intracellular accumulation of $ICT2552^{act}$ in ICT2588-treated HT1080 cells was observed to be relatively gradual and slower compared to the rapid, relatively high accumulation in ICT2552-treated HT1080 cells (Fig. 1F).

3.2. Selective MT1-MMP inhibition blocks ICT2588 metabolism

We further confirmed the role of MT1-MMP in the cellular activation of ICT2588 by evaluating the degree of $ICT2552^{act}$ release and related metabolites following ICT2588 metabolism in the presence of various protease inhibitors; ilomastat and phosphoramidon (broad spectrum MMP inhibitors [20,21]), leupeutin (serine protease inhibitor [22]), and actinonin (reported to inhibit mutliple MMP enzymes, but not MT1-MMP [23]). Activation of ICT2588 was significantly inhibited by ilomastat and phosphoramidon (92% and 76% respectively, compared to control) in HT1080 cells, while leupeutin and actinonin demonstrated no significant effect. However, despite the observed lack of an inhibitory effect on the activation of ICT2588 by actinonin, relatively less $ICT2552^{act}$ (20% compared to the control) was released in addition to an observed major metabolite, Tyr-$ICT2552^{act}$. This can be explained by the fact that actinonin also inhibits aminopeptidase activity [24], which is

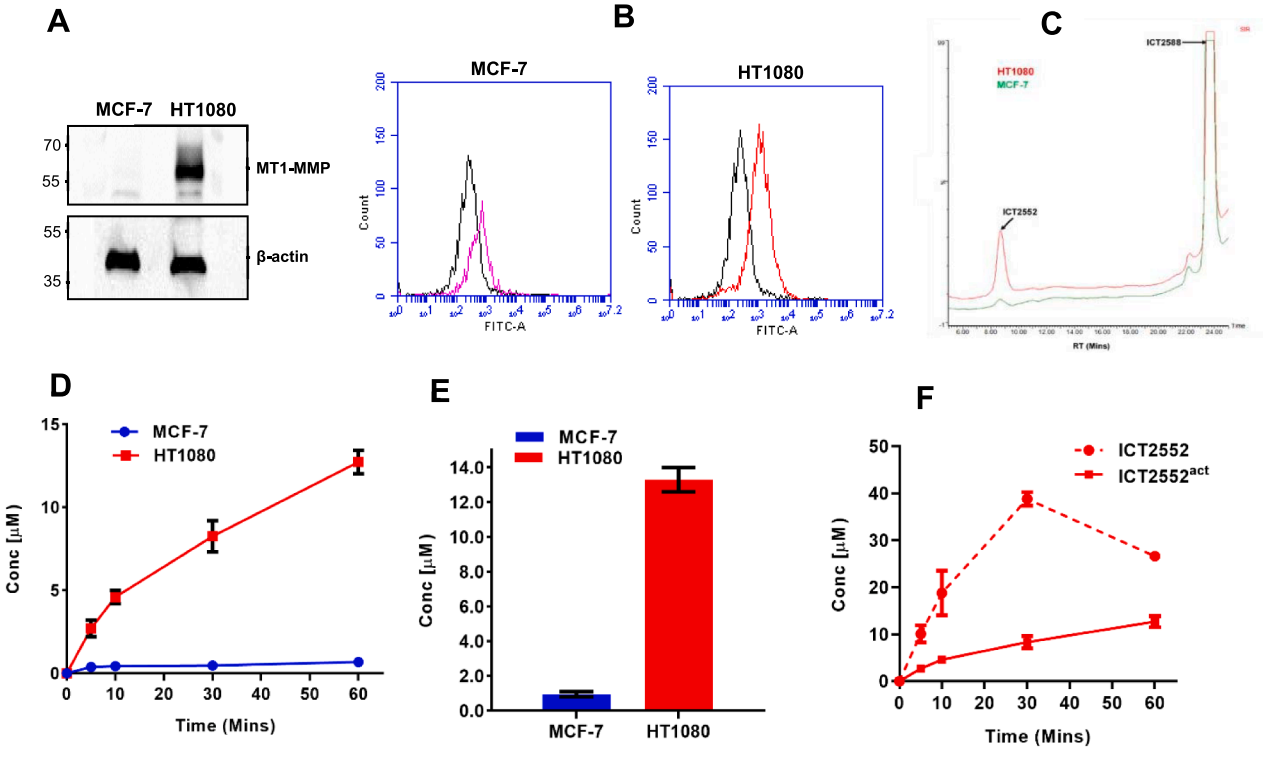

Fig. 1. MT1-MMP protein expression in MCF-7 (MT1-MMP negative) and HT1080 (MT1-MMP positive) cells, and cellular prodrug activation of ICT2588. Immunoblotting (A) and flow cytometry (B) analysis of MT1-MMP expression in MCF-7 and HT1080 cells. Selective Ion Recording (SIR) chromatogram: comparison of ICT2588 prodrug activation and release of $ICT2552^{act}$ in HT1080 and MCF-7 cells (C). *In-vitro* intracellular concentration of released active metabolite, $ICT2552^{act}$, following ICT2588 activation (and subsequent metabolism) by MCF-7 cells and HT1080 cells with time (D). Differential of release (10-fold) of $ICT2552^{act}$ due to selective activation of ICT2588 in HT1080 cells over MCF-7 cells after 60 min incubation (E). $ICT2552^{act}$ cellular release and accumulation profile characteristics in ICT2588-treated HT1080 cells compared to ICT2552-treated HT1080 cells at equimolar concentration (F). Data shown are the mean of > 3 independent experiments ± SEM. **** $p > 0.0001$.

required for the release of ICT2552^{act} from Tyr-ICT2552^{act} (Fig. 2).

3.3. MT1-MMP expression correlates with ICT2588 cytotoxicity

We then evaluated the correlation between MT1-MMP protein expression and cytotoxity in cell lines with relatively high (HT1080), low (MDA-MB-321) and negative (MCF-7) MT1-MMP expression. Selective cytotoxicity of ICT2588 was observed only in MT1-MMP positive cell lines (HT1080 and MDA-MB-231), and not the MT1-MMP negative cell line (MCF-7), while active agent ICT2552 demonstrated cytotoxicity in all cell lines, since MT1-MMP activity is not required in this case (Fig. 3; Table 1). The observed cytoxicity of ICT2558 correlated with MT1-MMP expression, and also was consistent with the selective activation of ICT2588 observed in MT1-MMP positive cells. While the data agree with previous studies investigating ICT2588 activation *ex-vivo* [8,9], this further establishes that the cellular uptake mechanisms for ICT2588 do not compromise its activation and subsequent metabolism by MT-MMP positive cells to release the active drug.

3.4. Effect of ICT2588 on cell cycle and apoptosis

ICT2588 has already been shown to cause tubulin disruption and vasculature collapse in MT1-MMP positive tumours *in vivo* [8]. However, colchicine and its derivatives are known to induce G2/M arrest, and trigger apoptosis [5,25] in cancer cells. The effect of ICT2588 on cell cycle progression and apoptosis was analysed in HT1080 (MT1-MMP positive) and MCF-7 (MT1-MMP negative) cells. Treatment of ICT2588 in HT1080 cells resulted in significant G2/M arrest (51.1% vs. 15.6% for control, $P < 0.0001$) which was comparable to G2/M arrest (57.2% vs. 15.6% for control, $P < 0.0001$) observed for treatment with ICT2552 (Fig. 4A & B). Conversely, G2/M arrest was only observed in MCF-7 cells (66.1% vs 18.8% for control, $P < 0.0001$) following treatment with ICT2552, and not ICT2588 (17.4% vs 18.8% for control, Fig. 4D & E).

The apperance a sub-G1 population is an indication of DNA damage and degradation during apoptosis [26]. We therefore quantified the percentage of sub-G1 cells as an indication of apoptosis. As shown in Fig. 4C, treatment with either prodrug ICT2588 or active drug ICT2552 triggered a significant and comparable increase in apoptosis (approx. 30% vs 4.9% for control, $P < 0.0001$) in HT1080 cells. However, signs of apoptosis were only observed following treatment with ICT2552 in MCF-7 cells (Fig. 4F).

Caspase activity is notably required for apoptotic events and cell death, with caspase-3 frequently activated in mammalian cell apoptosis [27]. To confirm the observed apoptosis associated with ICT2588 in HT1080 cells, we investigated the presence of activated caspase-3 and cleavage of its substrate poly(ADP-ribose) polymerase (PARP) in HT1080 cells treated either with ICT2588 or ICT2552. Cleaved caspase-3 (indicative of caspase activation) and cleavage of PARP were both detected by western blot in HT1080 cells but not in MCF-7 cells following treatment with ICT2588 (Fig. 4G).

3.5. ICT2588 provides synergistic activity with ATR inhibitor AZD6738

ATR is the principal mediator of the intra S-checkpoint and G2/M checkpoint of the cell cycle such that emerging evidence has demonstrated synergistic activity between ATR inhibitors and DNA damaging agents [12]. As shown earlier, the colchicine analogue ICT2552 and its prodrug ICT2588 both induce apoptosis in MT1-MMP-expressing cancer cells. DNA damage is a known signal for the initiation of apoptosis [26]. In addition, ATR has been described to have a replication-independent role in mitosis [28], a process known to be disrupted by colchicine analogues. We therefore evaluated the potential synergistic activity between ICT2588 (and ICT2552) with AZD6738 (an ATR inhibitor) in MT1-MMP positive cells by determining synergy score using Synergy Finder (https://synergyfinder.fimm.fi) following 72 h treatment in a 2-dimensional dosing matrix.

Using both ZIP and HSA Synergy Score, we observed a strong synergetic interaction between prodrug ICT2588 and AZD6738 over wide range of concentration combinations in HT1080 (Fig. 5) and MDA-MB-231 cells (Fig. 6). ICT2588 at concentrations below its IC_{50}, particularly at 100 nM (0.58 × IC_{50}) in combination with non-toxic concentrations of AZD6738 (0.002 × IC_{50} – 0.2 × IC_{50}) exhibited high ZIP synergy scores; 28.4 – 38.4. (Fig. 5A & C) in HT1080 cells, indicating profound synergism, and as shown by the growth curves (Fig. 5D & E), the strong synergistic cytotoxic effect of the AZD6738 and ICT2588 combination

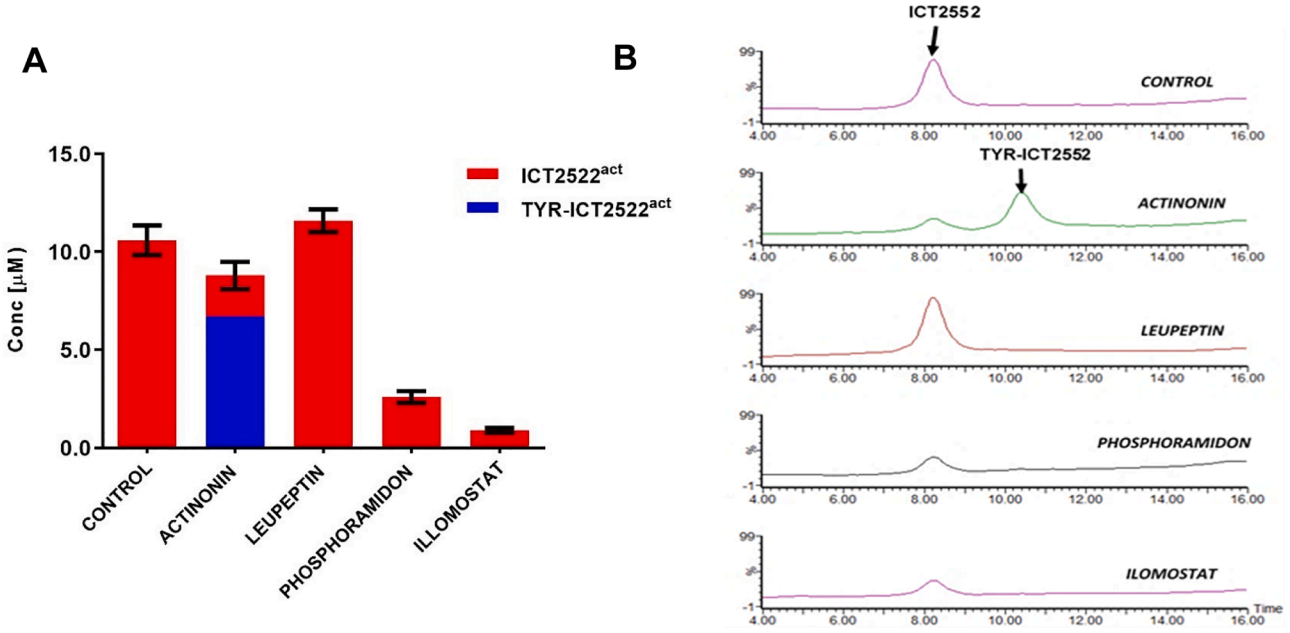

Fig. 2. *In-vitro* protease inhibition of ICT2588 activation. (A) Release of ICT2552^{act} following MT1-MMP-mediated activation of ICT2588 was inhibited only by ilomastat and phosphoramidon (broad spectrum MMP inhibitors), but not by leupeptin (serine protease inhibitor) or actinonin (broad-spectrum MMP inhibitor that does not inhibit MT1-MMP). All inhibitors were used at a concentration 100 μM (B). Data shown are the mean of > 3 independent experiments ± SEM.

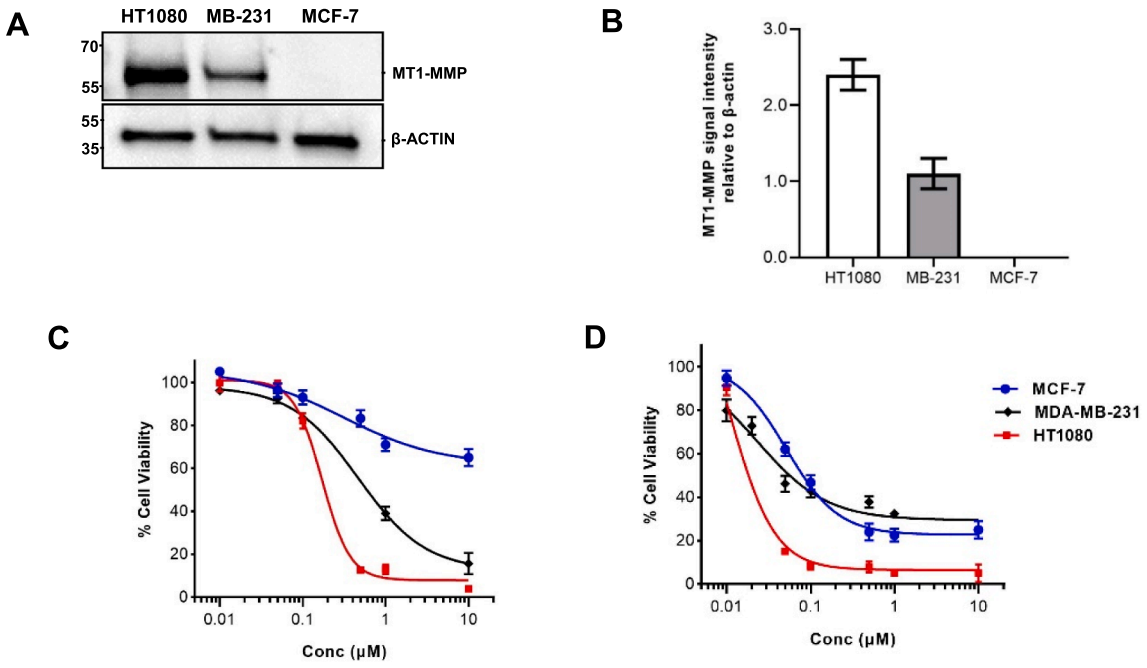

Fig. 3. MT1-MMP expression correlates with ICT2588 cytotoxicity. (A) MT1-MMP expression in cancer cell lines was analysed by western blotting. (B) Relative expression of MT1-MMP in cancer cell lines; band intensity was measured by Image Lab Software 6.1 and normalised to a β-actin loading control. HT1080, MDA-MB-231 and MCF-7 cells were treated with various concentrations of ICT2588 (C) and ICT2552 (D) for 72 h, and cell viability was assessed via an MTT assay. Data shown are the mean of > 3 independent experiments ± SEM. $p < 0.0001$.

Table 1
Growth inhibition of MCF-7, MDA-MB-231 and HT1080 cells following treatment with ICT2552, ICT2558 or AZD6738.

		IC_{50} (nM)		
		24 h	*48 h*	*72 h*
HT1080	ICT2552	42.4 ± 7.2	32.6 ± 5.2	29.5 ± 6.8
	ICT2588	556 ± 35	174 ± 25	150 ± 23
	AZD6738	>10,000	ND	4,597 ± 416
MB-231	ICT2552	88.6 ± 12.9	ND	45.2 ± 4.0
	ICT2588	2,108 ± 123	ND	362 ± 40
	AZD6738	>10,000	ND	2,912 ± 878
MCF-7	ICT2552	83.9 ± 11.4	58.8 ± 13.0	57.3 ± 8.1
	ICT2588	>10,000	>10,000	>10,000

significantly decreased the IC_{50}, compared to treatment with either agent alone. Similar results were observed in MDA-MB-231 cells, with a highest ZIP synergy score of 21.0 at concentrations of 0.13 × IC_{50} of ICT2588, and 0.03 × IC_{50} of AZD6738 respectively when in combination (Fig. 6A &C).

Interestingly, the combination of AZD6738 and active drug ICT2552 showed either no synergy or antagonistic activity, with overall ZIP synergy scores of −3.7 and −3.9, over a wide range of concentration combinations for HT1080 and MB-231 cells respectively (Fig. 5B & 6B). This observation was consistent with the reported lack of synergistic activity between AZD6738 and docetaxel (also a tubulin-binding agent, like ICT2552) [15].

3.6. The combination of ICT2588 and AZD6738 induces DNA damage and cell death

To understand the mechanisms accounting for the observed synergism between ICT2588 and AZD6738, we analysed proteins associated with DDR mechanisms, particularly the ATR-CHK1 pathway at the combination with the highest ZIP synergy after 72 h treatment, namely AZD6738 (1.0 μM) and ICT2588 (100 nM) for HT1080 cells (Fig. 5A), and AZD6738 (0.1 μM) and ICT2588 (50 nM) for MB-231 cells (Fig. 6A). ICT2588 monotherapy was observed to induce $CHK1^{S345}$ phosphorylation in HT1080 cells, an indication of DDR activation in response to DNA damage, although the observed ICT2588-induced DNA damage seemed insufficient to induce γH2AX phosphorylation, a molecular marker of DNA damage [29] or to induce apoptosis (a lack of cleaved caspase-3 and PARP expression observed). However, in the presence of a non-toxic concentration of AZD6738 (0.2 × IC_{50}, 1.0 μM), the ICT2588-induced CHK1 phosphorylation was blocked, leading to a high levels of γH2AX phosphorylation (>10-fold), suggesting a profound increase of DNA damage particularly double-strand breaks (DSBs). Consequently, increased cleaved caspase-3 and PARP was observed, with the combination of both drugs indicating increased apoptosis (Fig. 7A). In addition, using a phospho-ATM/ATR (S*Q) multiple substrate antibody, the combination of both drugs was observed to increase the phosphorylation of ATR/ATM substrates, as compared to ICT2588 monotherapy (Fig. 7C).

We further studied the effect of the ICT2588 and AZD6738 combination on cell cycle progression after 72 h treatment. The combination treatment was observed to significantly reduce the G1 cell population (53.3% vs. 65.9% for control, $P < 0.0001$ and to increase apoptosis (22.7% vs. 6.1% for control, $P < 0.0001$), while monotherapy of both agents showed no significant difference in G1 populations compared to control, with less or no indication of increased apoptosis (Fig. 7D).

4. Discussion

VDAs such colchicine represent an effective chemotherapeutic class of anti-cancer agent with significant potential, but systemic toxicities continue to hinder their clinical progression [6,7]. ICT2588, a prodrug of azademethylcolchicine, is representative of a promising therapeutic strategy to overcome these limitations [8,9]. The previously reported preclinical data for ICT2588 primarily explored the selectivity of its tumour vascular disrupting ability and subsequent antitumour activity *in vivo*, while in addition to its vascular disrupting properties, colchicine and its derivatives are also known to induce G2/M arrest, DSB DNA damage and to trigger apoptosis [3,5]. In this present study, the cellular

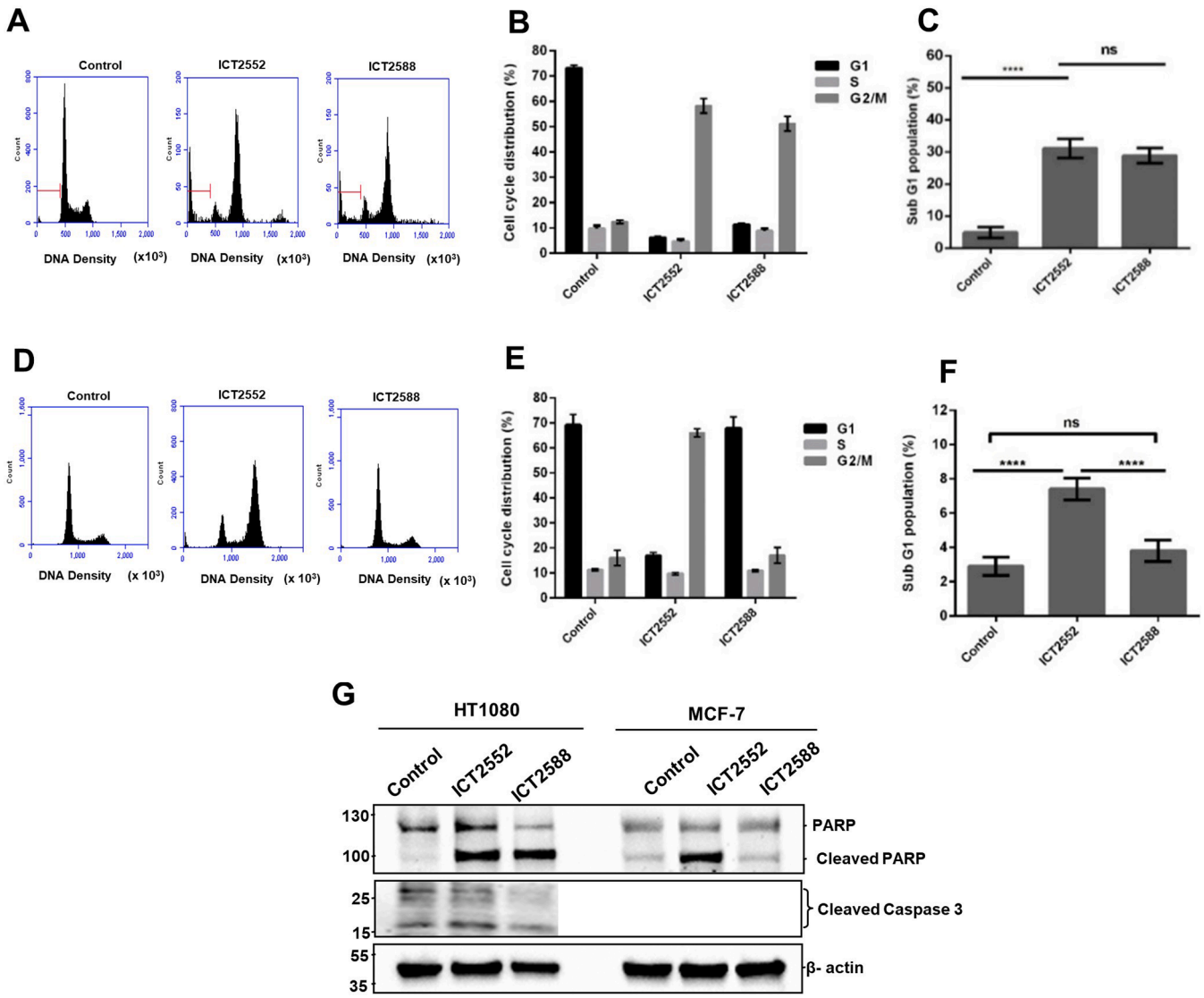

Fig. 4. Differential effects of ICT2588 on cell cycle distributions in HT1080 and MCF-7 cells. Representative flow cytometric analyses of HT1080 (A) and MCF-7 (B) cells. Cells were incubated with ICT2552 or ICT2588 at their IC_{50} concentrations for 24 h. The cells were then fixed with 66% ethanol and stained with propidium iodide. Cell cycle distributions of HT1080 (B) and MCF-7 (D) cells, after treatment with ICT2552 and ICT2558. The percentage of apoptosis (sub-G1 population) induced by ICT2552 and ICT2558 in HT1080 (E) and MCF-7 (F) cells. HT1080 and MCF-7 cells were cultured with ICT2552 and ICT2588 at their IC_{50} concentrations for 24 h, and cell lysates were analysed by western blotting with anti-PARP / cleaved PARP, anti-cleaved caspase-3 antibodies. **** $p > 0.0001$.

activation of ICT2588, its effects on cell cycle progression, and potential synergism with ATR inhibition were explored.

Consistent with the previously published selective tumour metabolism of ICT2588 *ex vivo* [8], we have shown that MT1-MMP expression is critical for the cellular prodrug activation of ICT2588, with release of its active warhead ($ICT2552^{act}$) not hindered by uptake into cancer cells and subsequent metabolism mechanisms essential for the prodrug. One challenge limiting the efficiency of many peptide prodrugs is poor or slow release of the active drug from peptidyl-related metabolites after having been differentially activated at the target site [30]. Our data demonstrated that no such metabolites remain following activation of the prodrug, with only active azademethylcolchicine ($ICT2552^{act}$) detected intracellularly consequent to ICT2588 activation and subsequent peptide metabolism. However, the rate of release and intracellular accumulation of $ICT2552^{act}$ was demonstrated to be relatively slow in contrast to the rapid high intracellular accumulation when ICT2552 was administered directly. This observation perhaps explains the relatively delayed cytotoxic activity of the prodrug (ICT2588) on MT1-MMP-expressing cells compared to the active warhead (ICT2552), as intracellular concentrations of drugs strongly impact on their cytotoxicity [31,32]. We have also demonstrated the dependency on MT1-MMP expression levels to the chemosensitivity of the prodrug *in vitro*, since cells with higher expression of MT1-MMP protein (HT1080) were more chemosensitive compared to cells with relatively lower levels of MT1-MMP expression (MDA-MB-231). This once again confirms the selectivity of ICT2588, and that its activation is mediated by MT1-MMP activity.

We have, for the first-time, demonstrated the effects of ICT2588 and its active metabolite ($ICT2552^{act}$) on cancer cell cycle progression. ICT2588 was demonstrated to halt cell cycle progression at the G2/M phase, and triggers apoptosis in MT1-MMP-expressing cells, in a manner similar to that with the active drug ICT2552, perhaps contributing to its reported potency both *in vitro* and *in vivo* [8–10]. The observed PARP degradation and DNA fragmentation associated with the ICT2552-induced apoptosis suggests that the mechanism of this apoptosis is associated with caspase activation [5,33], which is inconsistent with previous studies associated with many tubulin binding agents, including colchicine derivatives [34].

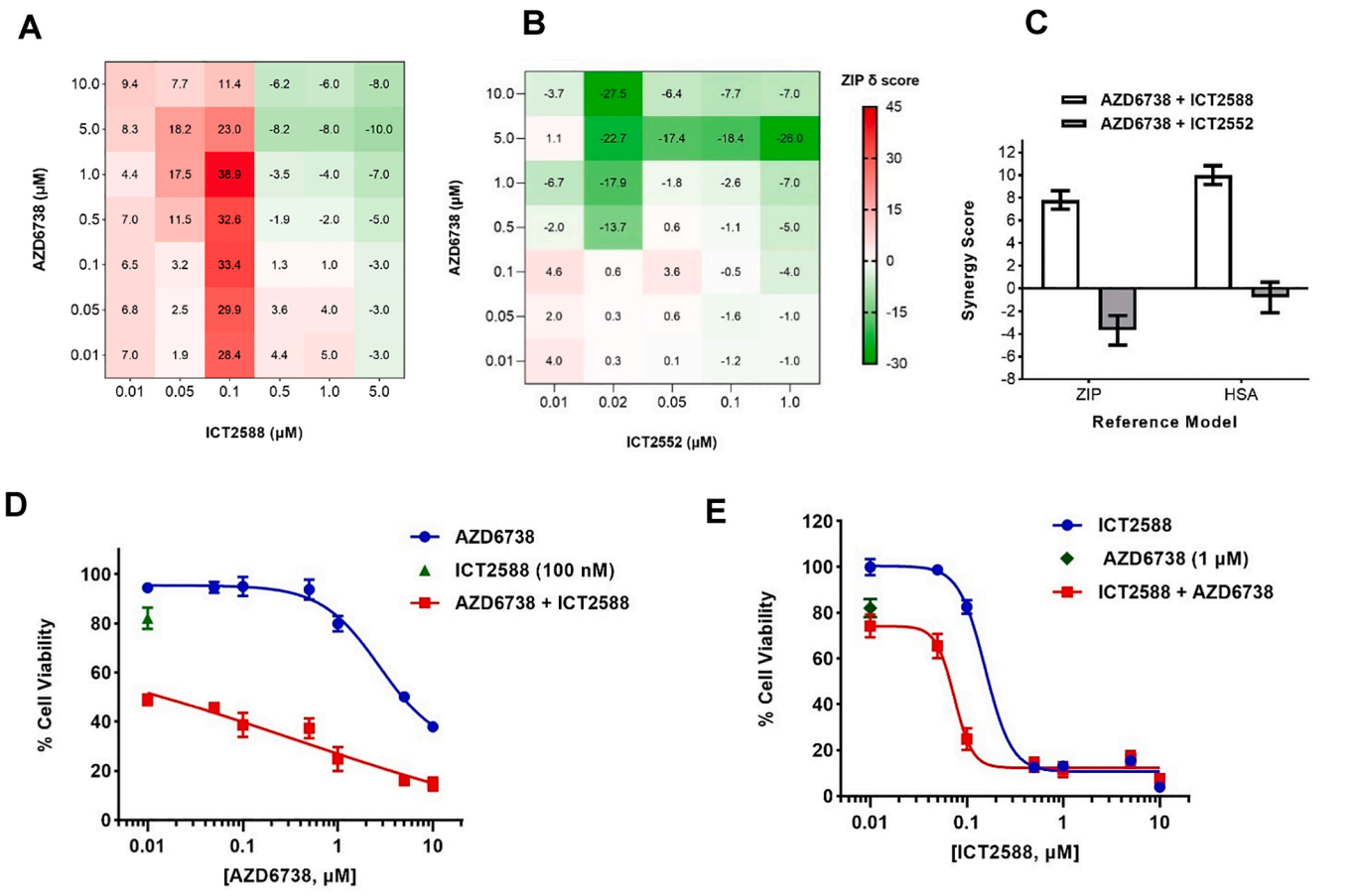

Fig. 5. AZD6738 shows a synergistic effect with ICT2588 (A), but not with ICT2552 (B), in HT1080 cells. Synergy score (ZIP) as indicated in the colour-coded matrix was calculated using Synergy Finder (https://synergyfinder.fimm.fi). Synergy scores indicate the interactions between the two drugs, indicating antagonism (scores less than − 10), addition (scores from − 10 to 10), or synergism (scores>10). Overall synergy score of the matrix, using 2 different reference models (C). HT1080 cells were treated with various concentrations of AZD6738, combined with a fixed concentration of ICT2588 (D), and various concentrations of ICT2588 were combined with a single concentration of AZD6738 (E) for 72 h, and cell viability was assessed via an MTT assay. Data shown are the mean of 3 independent experiments ± SEM.

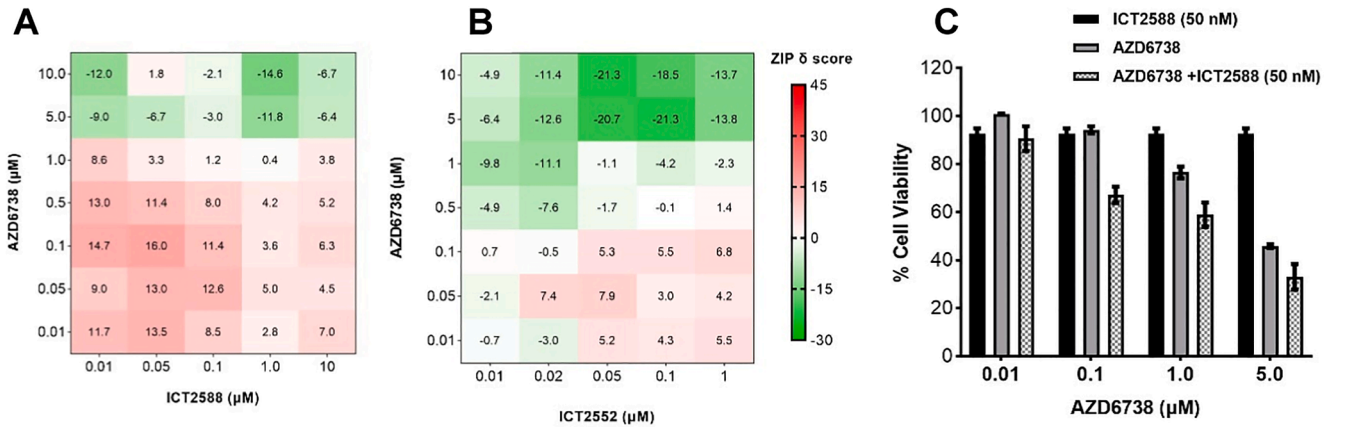

Fig. 6. AZD6738 shows synergism with ICT2588 (A), but not with ICT2552 (B) in MDA-MB-231 cells after 72 h treatment. Synergy score (ZIP), as indicated in the colour coded matrix, was calculated using Synergy Finder (https://synergyfinder.fimm.fi). Synergy scores indicate the interactions between the two drugs: antagonism (scores less than − 10), addition (scores from − 10 to 10), or synergism (scores>10); MDA-MB-231 cells were treated with a range of concentrations of AZD6738 combined with a single ICT2588 concentration (50 nM) for 72 h, and cell viability was assessed by MTT assay (C); Combination of ICT2588 and AZD6738 induces DNA damage and cell death. Data shown are the mean of 3 independent experiments ± SEM.

ATR is one of the two main regulators of the DDR pathway that coordinates cellular responses to DNA damage, and is critical for the survival of cancer cells due high replication stress and self-inflicted DNA damage associated these cells [12]. However, the sensitivity of ATR inhibitors has been demonstrated to be associated ATM loss [35,36], hence it was not surprising that both HT1080 and MDA-MB-231 cells were shown to be insensitive (IC_{50} > 1.0 μM) to AZD6738 (ATR inhibitor) treatment after 72 h, since both cells line are ATM-competent. We have, however, demonstrated that despite the apparent insensitivity of these cells to AZD6738 monotherapy, that addition of the prodrug

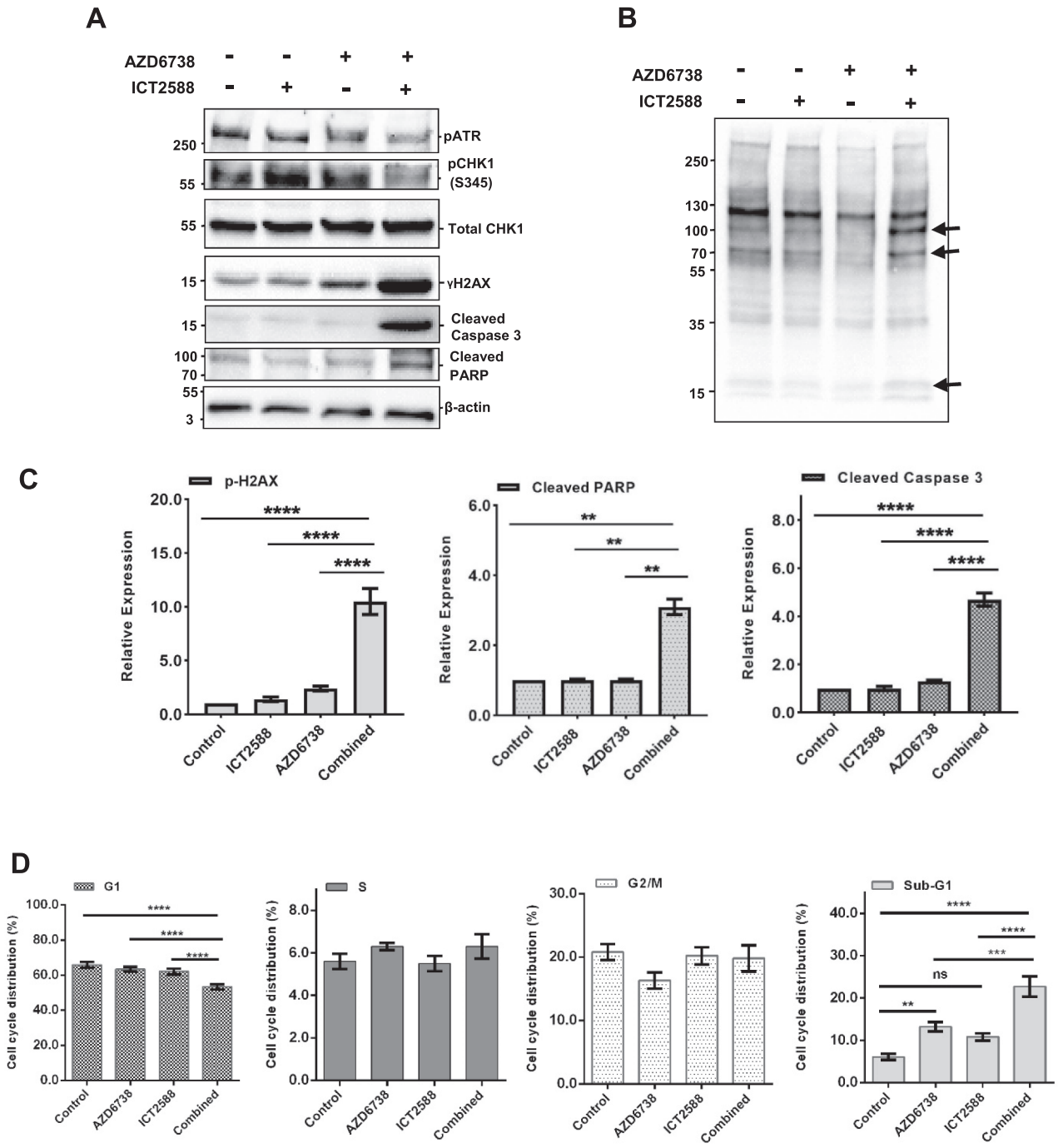

Fig. 7. A combination of ICT2588 and AZD6738 (induces DNA damage and cell death. HT1080 cells were cultured with ICT2558 (100 nM) and AZD6738 (1.0 μM) for 72 h, and cell lysates were analysed by western blotting for pATR, pCHK1S345, total CHK1, γH2AX, cleaved caspase-3 and cleaved PARP protein expression (A), and multiple phospho-ATR/ATM substrates (B); Relative expression of γH2AX, cleaved PARP, and cleaved caspase-3 (C). Mean fold-change in protein band intensity was measured by Image Lab Software 6.1, and normalised to a β-actin loading control. Effects of AZD6738 and ICT2588 combinations on cell cycle progression of HT1080 cells (D). Data shown are the mean of 3 independent experiments ± SEM. ** $p > 0.01$ and **** $p > 0.0001$.

ICT2588 potentiated AZD6738 activity and *vice versa* in these cells. This was not the case for the combination of AZD6738 and the active warhead (ICT2552), an observation which is consistent with the published lack of synergistic activity between AZD6738 and docetaxel (also a tubilin binding agent) [15].

The observed synergism between AZD6738 and the prodrug ICT2588, but not its active warhead ICT2552, can be attributed to the differential intracellular accumulation pattern of the potent colchicine analogue in ICT2588-treated and ICT2552-treated cancer cells as we have demonstrated. Unlike the rapid high intracellular accumulation of ICT2552 in ICT2552-treated cells which correlated to its low IC_{50}, a delayed but sustained gradual increase of $ICT2552^{act}$ release and intracellular accumulation was observed following administration of the compound as the prodrug ICT2588. This sustained pattern of release and accumulation of $ICT2552^{act}$ though not sufficient for cytotoxic activity at low concentrations appears to cause DNA damage, which is sufficient to activate the ATR pathway. This is supported by our data. As we have demonstrated, the monotherapy of both ICT2588 and AZD6738 at non-

toxic concentrations showed no significant cell death and apoptosis, but the *combination* of AZD6738 and ICT2588 induced the high levels of gamma-H2AX phosphorylation and expression of apoptotic markers observed. This suggests that ICT2588 monotherapy at non-toxic concentrations, though not causing G2/M arrest (as confirmed by cycle analysis) and cell death, causes sustained and prolonged DNA damage (a probable reflection of the sustained gradual increase of ICT2552^{act} release and accumulation following prodrug activation) which is compensated for by ATR activity (as evidenced by the increased phosphorylation of CHK1). The inhibition of ATR therefore seems to potentiate the effect of this ICT2588-induced DNA damage, leading to accumulation of lethal DNA DSBs and cell death [14], perhaps explaining the observed synergism between ICT2588 and AZD6738 at non-toxic concentrations.

Also, the observation of differential phosphorylation of ATR/ATM substrates with the combination treatment suggests activation of ATM in response to ICT2588-induced DNA damage in the absence of ATR activity, although perhaps insufficient to compensate for the loss of ATR function in the DDR following ICT2588 metabolism. This implies that though other DDR checkpoints besides ATR are likely to be activated in response to ICT2588-induced DNA damage, the combination of ICT2588 and ATR inhibitor is likely to be beneficial.

In conclusion, we have demonstrated that prodrug ICT2588 is activated by only MT1-MMP expressing tumour cells, with release of a potent colchicine analogue that induces G2/M arrest and apoptosis. In addition, the sustained gradual increase in the release and intracellular accumulation of the potent colchicine analogue (ICT2552) subsequent to activation and metabolism of ICT2588 (contrary to rapidly high intracellular drug accumulation subsequent to direct ICT2552 incubation) provided synergistic activity with ATR inhibition in a way not observed with the active drug (ICT2552). Given that VDAs have yet to fulfil their therapeutic potential, this *in vitro* data has important implications for possible combinations of targeted prodrug ICT2588 and DNA damage repair inhibitors in the clinic.

CRediT authorship contribution statement

Francis M. Barnieh: Conceptualization, Methodology, Investigation, Validation, Writing – original draft. **Goreti Ribeiro Morais:** Investigation. **Herbie Garland:** Investigation. **Paul M. Loadman:** Validation, Writing – review & editing. **Robert A. Falconer:** Conceptualization, Methodology, Supervision, Resources, Validation, Writing – review & editing.

Declaration of Competing Interest

The authors declare that they have no known competing financial interests or personal relationships that could have appeared to influence the work reported in this paper.

Acknowledgements

The authors thank the Ghana Educational Trust Fund for sponsoring FMB during his PhD studies. FMB is currently supported by a University of Bradford STARTER fellowship. Ms. Enrica Denasio is thanked for technical assistance with flow cytometry experiments.

References

[1] K.J. Bayless, G.A. Johnson, Role of the cytoskeleton in formation and maintenance of angiogenic sprouts, J Vasc Res 48 (5) (2011) 369–385.
[2] G.M. Tozer, C. Kanthou, B.C. Baguley, Disrupting tumour blood vessels, Nat Rev Cancer 5 (6) (2005) 423–435.
[3] Z. Mao, M. Bozzella, A. Seluanov, V. Gorbunova, DNA repair by nonhomologous end joining and homologous recombination during cell cycle in human cells, Cell Cycle 7 (18) (2008) 2902–2906.
[4] E. Bonfoco, S. Ceccatelli, L. Manzo, P. Nicotera, Colchicine induces apoptosis in cerebellar granule cells, Exp Cell Res 218 (1) (1995) 189–200.
[5] S.-K. Kim, S.-M. Cho, H.o. Kim, H. Seok, S.-O. Kim, T. Kyu Kwon, J.-S. Chang, The colchicine derivative CT20126 shows a novel microtubule-modulating activity with apoptosis, Experimental & Molecular Medicine 45 (4) (2013).
[6] M.M. Mita, L. Sargsyan, A.C. Mita, M. Spear, Vascular-disrupting agents in oncology, Expert Opinion on Investigational Drugs 22 (3) (2013) 317–328.
[7] W.J. van Heeckeren, S. Bhakta, J. Ortiz, J. Duerk, M.M. Cooney, A. Dowlati, K. McCrae, S.C. Remick, Promise of new vascular-disrupting agents balanced with cardiac toxicity: is it time for oncologists to get to know their cardiologists? J Clin Oncol 24 (10) (2006) 1485–1488.
[8] J.M. Atkinson, R.A. Falconer, D.R. Edwards, C.J. Pennington, C.S. Siller, S. D. Shnyder, M.C. Bibby, L.H. Patterson, P.M. Loadman, J.H. Gill, Development of a Novel Tumor-Targeted Vascular Disrupting Agent Activated by Membrane-Type Matrix Metalloproteinases, Cancer Res 70 (17) (2010) 6902–6912.
[9] J.H. Gill, P.M. Loadman, S.D. Shnyder, P. Cooper, J.M. Atkinson, G. Ribeiro Morais, L.H. Patterson, R.A. Falconer, Tumor-Targeted Prodrug ICT2588 Demonstrates Therapeutic Activity against Solid Tumors and Reduced Potential for Cardiovascular Toxicity, Molecular Pharmaceutics 11 (4) (2014) 1294–1300.
[10] C. Ansari, G.A. Tikhomirov, S.H. Hong, R.A. Falconer, P.M. Loadman, J.H. Gill, R. Castaneda, F.K. Hazard, L. Tong, O.D. Lenkov, D.W. Felsher, J. Rao, H. E. Daldrup-Link, Development of novel tumor-targeted theranostic nanoparticles activated by membrane-type matrix metalloproteinases for combined cancer magnetic resonance imaging and therapy, Small 10 (3) (2014) 566–575.
[11] L. Carrassa, G. Damia, DNA damage response inhibitors: Mechanisms and potential applications in cancer therapy, Cancer Treatment Reviews 60 (2017) 139–151.
[12] F.M. Barnieh, P.M. Loadman, R.A. Falconer, Progress towards a clinically-successful ATR inhibitor for cancer therapy, Current Research in Pharmacology and Drug Discovery 2 (2021) 100017, https://doi.org/10.1016/j.crphar.2021.100017.
[13] M.SY. Huen, J. Chen, The DNA damage response pathways: at the crossroad of protein modifications, Cell Research 18 (1) (2008) 8–16.
[14] K.A. Cimprich, D. Cortez, ATR: an essential regulator of genome integrity, Nature Reviews Molecular Cell Biology 9 (8) (2008) 616–627.
[15] F.P. Vendetti, A. Lau, S. Schamus, T.P. Conrads, M.J. O'Connor, C.J. Bakkenist, The orally active and bioavailable ATR kinase inhibitor AZD6738 potentiates the anti-tumor effects of cisplatin to resolve ATM-deficient non-small cell lung cancer in vivo, Oncotarget 6 (42) (2015) 44289–44305.
[16] J. Hur, M. Ghosh, T.H. Kim, N. Park, K. Pandey, Y.B. Cho, S.D. Hong, N.B. Katuwal, M. Kang, H.J. An, Y.W. Moon, Synergism of AZD6738, an ATR Inhibitor, in Combination with Belotecan, a Camptothecin Analogue, in Chemotherapy-Resistant Ovarian Cancer, Int J Mol Sci 22 (3) (2021) 1223, https://doi.org/10.3390/ijms22031223.
[17] Y. Wallez, C.R. Dunlop, T.I. Johnson, S.B. Koh, C. Fornari, J.W.T. Yates, B. de Quirós, S. Fernández, A. Lau, F.M. Richards, D.I. Jodrell, The ATR Inhibitor AZD6738 Synergizes with Gemcitabine In Vitro and In Vivo to Induce Pancreatic Ductal Adenocarcinoma Regression, Mol Cancer Ther 17 (2018) 1670–1682.
[18] M. Jove, J.A. Spencer, M.E. Hubbard, E.C. Holden, R.D. O'Dea, B.S. Brook, R. M. Phillips, S.W. Smye, P.M. Loadman, C.J. Twelves, Cellular uptake and efflux of palbociclib in vitro in single cell and spheroid models, Journal of Pharmacology and Experimental Therapeutics 370 (2) (2019) 242–251.
[19] L. Devy, L. Huang, L. Naa, N. Yanamandra, H. Pieters, N. Frans, E. Chang, Q. Tao, M. Vanhove, A. Lejeune, R. van Gool, D.J. Sexton, G. Kuang, D. Rank, S. Hogan, C. Pazmany, Y.L. Ma, S. Schoonbroodt, A.E. Nixon, R.C. Ladner, R. Hoet, P. Henderikx, C. TenHoor, S.A. Rabbani, M.L. Valentino, C.R. Wood, D. T. Dransfield, Selective Inhibition of Matrix Metalloproteinase-14 Blocks Tumor Growth, Invasion, and Angiogenesis, Cancer Res 69 (4) (2009) 1517–1526.
[20] A. Veerendhar, R. Reich, E. Breuer, Phosphorus based inhibitors of matrix metalloproteinases, Comptes Rendus Chimie 13 (8-9) (2010) 1191–1202.
[21] M. Yamamoto, H. Tsujishita, N. Hori, Y. Ohishi, S. Inoue, S. Ikeda, Y. Okada, Inhibition of membrane-type 1 matrix metalloproteinase by hydroxamate inhibitors: an examination of the subsite pocket, J Med Chem 41 (1998) 1209–1217.
[22] L. Hedstrom, T.-Y. Lin, W. Fast, Hydrophobic Interactions Control Zymogen Activation in the Trypsin Family of Serine Proteases, Biochemistry 35 (14) (1996) 4515–4523.
[23] R.C. Wahl, T.A. Pulvino, A.M. Mathiowetz, A.K. Ghose, J.S. Johnson, D. Delecki, E. R. Cook, J.A. Gainor, M.R. Gowravaram, B.E. Tomczuk, Hydroxamate inhibitors of human gelatinase B (92 kDa), Bioorganic & Medicinal Chemistry Letters 5 (4) (1995) 349–352.
[24] R.J. Ganji, R. Reddi, R. Gumpena, A.K. Marapaka, T. Arya, P. Sankoju, S. Bhukya, A. Addlagatta, Structural basis for the inhibition of M1 family aminopeptidases by the natural product actinonin: Crystal structure in complex with E. coli aminopeptidase N, Protein Sci 24 (5) (2015) 823–831.
[25] K. Kowalczyk, A. Błauż, W.M. Ciszewski, A. Wieczorek, B. Rychlik, D. Plażuk, Colchicine metallocenyl bioconjugates showing high antiproliferative activities against cancer cell lines, Dalton Transactions 46 (48) (2017) 17041–17052.
[26] JYJ Wang, DNA damage and apoptosis, Cell Death & Differentiation 8 (11) (2001) 1047–1048.
[27] A.G. Porter, R.U. Jänicke, Emerging roles of caspase-3 in apoptosis, Cell Death Differ 6 (2) (1999) 99–104.
[28] L. Kabeche, H.D. Nguyen, R. Buisson, L. Zou, A mitosis-specific and R loop-driven ATR pathway promotes faithful chromosome segregation, Science 359 (6371) (2018) 108–114.
[29] L.-J. Mah, A. El-Osta, T.C. Karagiannis, γH2AX: a sensitive molecular marker of DNA damage and repair, Leukemia 24 (4) (2010) 679–686.
[30] D.G. Vartak, R.A. Gemeinhart, Matrix metalloproteases: underutilized targets for drug delivery, J Drug Target 15 (1) (2007) 1–20.

[31] C. Wu, X. Wang, M. Xu, Y. Liu, X. Di, Intracellular Accumulation as an Indicator of Cytotoxicity to Screen Hepatotoxic Components of Chelidonium majus L. by LC-MS/MS, Molecules 24 (13) (2019) 2410, https://doi.org/10.3390/molecules24132410.

[32] L. Tanner, G.T. Mashabela, C.C. Omollo, T.J. de Wet, C.J. Parkinson, D.F. Warner, R.K. Haynes, L. Wiesner, P.C. Karakousis, Intracellular Accumulation of Novel and Clinically Used TB Drugs Potentiates Intracellular Synergy, Microbiol Spectr 9 (2) (2021), https://doi.org/10.1128/Spectrum.00434-21.

[33] L.M. Mooney, K.A. Al-Sakkaf, B.L. Brown, P.R.M. Dobson, Apoptotic mechanisms in T47D and MCF-7 human breast cancer cells, British journal of cancer 87 (8) (2002) 909–917.

[34] K.N. Bhalla, Microtubule-targeted anticancer agents and apoptosis, Oncogene 22 (56) (2003) 9075–9086.

[35] M. Kwok, N. Davies, A. Agathanggelou, E. Smith, C. Oldreive, E. Petermann, G. Stewart, J. Brown, A. Lau, G. Pratt, H. Parry, M. Taylor, P. Moss, P. Hillmen, T. Stankovic, ATR inhibition induces synthetic lethality and overcomes chemoresistance in TP53- or ATM-defective chronic lymphocytic leukemia cells, Blood 127 (2016) 582–595.

[36] A. Min, S.-A. Im, H. Jang, S. Kim, M. Lee, D.K. Kim, Y. Yang, H.-J. Kim, K.-H. Lee, J. W. Kim, T.-Y. Kim, D.-Y. Oh, J. Brown, A. Lau, M.J. O'Connor, Y.-J. Bang, AZD6738, A Novel Oral Inhibitor of ATR, Induces Synthetic Lethality with ATM Deficiency in Gastric Cancer Cells, Mol Cancer Ther 16 (4) (2017) 566–577.